JOURNAL OF COORDINATION CHEMISTRY
2025, VOL. 78, NO. 19, 2212–2229
https://doi.org/10.1080/00958972.2025.2549144

Coordination complexes of *N*-((4-pyridyl)methyl)-1,8-naphthalimide and divalent metal halides: structures and solid-state fluorescence

B. M. Parveen Beebeejaun-Boodoo and Melanie Rademeyer

Department of Chemistry, University of Pretoria, Pretoria, South Africa

ABSTRACT

The coordination complexes formed between the fluorophore N-((4-pyridyl)methyl)-1,8-naphthalimide (**4-pn**) and a range of divalent metal halides were studied. Five new complexes, of the formula $[M(4\text{-pn})_2X_2]$, where M = metal ion and X = halido ligand were obtained from the combination of **4-pn** and the divalent metal halides ZnX_2 ($X = Br^-$ or I^-), CoX_2 ($X = Cl^-$ or Br^-) or HgI_2. These coordination complexes were characterized using elemental analysis, powder X-ray diffraction and single crystal X-ray diffraction. Three different structural types were obtained with the metal centers displaying a distorted tetrahedral geometry in all the structures, but showing different degrees of distortion. Solid-state fluorescence studies were also conducted on these complexes to explore the influence of both the metal ion and halido ligand on the photophysical properties of the complexes. The complex containing $ZnBr_2$ shows fluorescence enhancement relative to **4-pn**, emitting at a similar wavelength to the organic ligand. However, complexes containing Co(II) show fluorescence quenching, emitting at lower wavelengths compared to **4-pn**. The presence of iodido ligands or Hg(II) in the complexes drastically reduces the fluorescence emission of the complex.

GRAPHICAL ABSTRACT

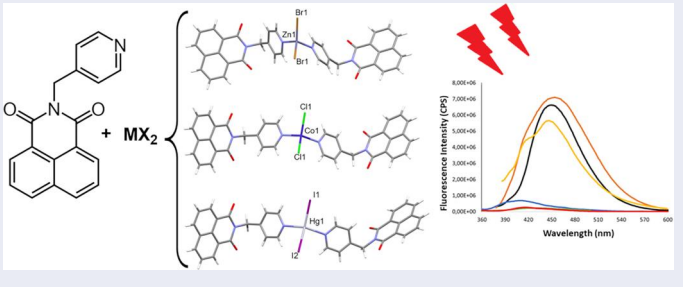

ARTICLE HISTORY
Received 14 May 2025
Accepted 11 August 2025

KEYWORDS
1,8-naphthalimide; coordination complexes; solid-state fluorescence

CONTACT B. M. Parveen Beebeejaun-Boodoo parveen.beebeejaun@up.ac.za Department of Chemistry, University of Pretoria, Pretoria, South Africa.

Supplemental data for this article can be accessed online at https://doi.org/10.1080/00958972.2025.2549144.

Introduction

Fluorescent materials play a significant role in scientific research due to their potential application in diverse fields, for example sensing, bio-imaging and optoelectronics [1]. 1,8-Naphthalimide derivatives are of interest as fluorescent materials since they have good photo-stability and show strong fluorescence, high fluorescence quantum yield [2] and tunable emission wavelength [3]. These properties, together with being both chemically and thermally stable, makes 1,8-naphthalimide derivatives ideal for use as colorants in the polymer industry [4] and fluorescence probes for medical and biological purposes [5]. 1,8-Naphthalimide derivatives can be designed in such a way to make standard light-emitting materials with a wide range of colors for applications as organic light emitting diodes (OLEDs) [6]. Applications of 1,8-naphthalimide derivatives also include fluorescent sensors [7], fluorescence cell markers [8], liquid crystal displays [9] and laser dyes [10].

The synthesis of coordination complexes containing the 1,8-naphthalimide moiety is of particular interest in this study. The organic ligand *N*-((4-pyridyl)methyl)-1,8-naphthalimide, abbreviated **4-pn**, used in the current study, was synthesized using conventional methodology by stirring equimolar quantities of 1,8-naphthalic anhydride with 4-(aminomethyl)pyridine in tetrahydrofuran as illustrated in Scheme 1 [11].

4-pn consists of three fused rings and a flexible (4-pyridyl)methyl arm, with the nitrogen atom of the pyridyl group acting as the coordination site. This ligand is of interest since it exhibits dual fluorescence due to the excited state with extended conjugation *via* π-stacking interactions, originating from charge transfer [12]. Molecules with dual fluorescence properties are used as analytical reagents for many substrates [13] and can also potentially be used as new lighting sources [14].

The crystal structure of the neutral organic ligand **4-pn** has been reported in the literature (Cambridge Structural Database, CSD [15]) with refcode WEZDAH [11]. We have previously reported the structures formed through the combination of **4-pn** and divalent metal halides under acidic conditions [16]. Under these acidic conditions, the **4-pn** ligand is protonated, to form a *N*-(4-picolinium)-1,8-naphthalimide cation, abbreviated as **pnH**, before the addition of the metal halide. Reaction with the metal halide then results in the formation of an ionic structure. In these ionic structures, tetrahalometallate anions adopt a tetrahedral geometry when the reaction was done with ZnX_2 ($X = Cl^-$ and Br^-), CoX_2 ($X = Cl^-$ and Br^-), $CdCl_2$ or $HgCl_2$, while the tetrahalocuprates, with CuX_2 ($X = Cl^-$ and Br^-), resulted in a distorted square planar geometry. A search of the CSD [15] (Version 5.45, September 2024 Update) revealed that no structures of coordination complexes containing the organic ligand **4-pn** with divalent metal halides have been reported in the literature. This indicated a gap in the literature leading to the current investigation, which focusses on the structural characterization and fluorescence study of coordination complexes formed between **4-pn** and a range of the metal halides. Coordination complexes of ((3-pyridyl)methyl)-1,8-naphthalimide with divalent metal halides CoX_2 and ZnX_2 ($X = Cl^-$ or Br^-) in different solvents have also been reported by our group, and all the complexes were found to contain solvent molecules in their crystal structures [17].

In the current study, the organic ligand **4-pn**, which is a fluorophore, was synthesized and complexed with a series of divalent metal halides to investigate their

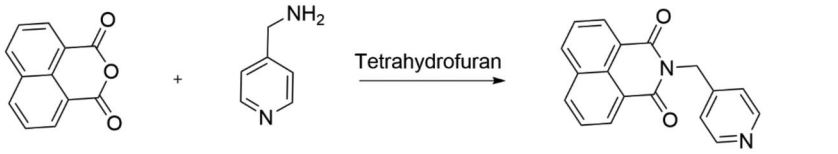

Scheme 1. The synthesis of *N*-((4-pyridyl)methyl)-1,8-naphthalimide**, 4-pn**

structures and the effect of the metal ion and halido ligand on the fluorescence properties of the complexes. Since paramagnetic metal ions were reported to enhance fluorescence while diamagnetic metal ions quench the fluorescence of a fluorophore [18], both paramagnetic (Co(II)) and diamagnetic metal ions (Zn(II) and Hg(II)) were used in this study.

Experimental

Chemicals and reagents

All starting materials and solvents were used as purchased without prior purification: $CoCl_2$ (98%, Fluka), $CoBr_2$ (98%, Sigma Aldrich), $ZnBr_2$ (99%, Riedel de Haen), ZnI_2 (99.9%, Sigma Aldrich), HgI_2 (99%, Sigma Aldrich), 4-(aminomethyl)pyridine (also known as 4-picolylamine) (98%, Sigma Aldrich), 1,8-naphthalic anhydride (95%, Sigma Aldrich), CH_3OH (99%, Merck), $CHCl_3$ (99.9%, Merck), THF (99.9%, Merck) and DMF (99%, Sigma Aldrich).

Synthesis

The yields of the reactions were not optimized.

Synthesis of N*-((4-pyridyl)methyl)-1,8-naphthalimide, 4-pn*

The organic ligand, **4-pn**, was prepared using the method described by Sarma *et al.* [11]. In our reaction, 5.0029 g (25.246 mmol) of 1,8-naphthalic anhydride and 2.7103 g (25.063 mmol) of 4-(aminomethy)pyridine were used. The method was adapted by recrystallizing the obtained solid from DMF. The experimental powder pattern of *N*-((4-pyridyl)methyl)-1,8-naphthalimide, **4-pn,** prepared in this study, matches the calculated powder pattern obtained from WEZDAH [11] and is shown in the Supplementary Information Section 1. Yield: 6.1868 g (85%).

Elemental Analysis for $C_{18}H_{12}N_2O_2$ (**4-pn**) (%): **Calcd.**: C, 74.99; H, 4.2; N, 9.72: **Found**: C, 73.78; H, 4.48; N, 9.24.

Synthesis of coordination complexes

The general synthetic method employed to prepare the coordination complexes **4-pnCoCl**, **4-pnCoBr**, **4-pnZnBr** and **4-pnHgI** involved the dissolution of the organic ligand, **4-pn**, in 10 ml of $CHCl_3$. This solution was placed in a vial, and a buffer layer of CH_3OH (3 ml) was carefully layered over the ligand solution. A solution of MX_2, in

10 ml of CH_3OH, was then layered over the buffer layer, and the vial was closed. The layered reaction was left undisturbed at room temperature, allowing the product to form at the interface. After two to three weeks, crystals of the product were harvested. The relevant synthetic information is given in Table 1.

The coordination complex **4-pnZnI** was prepared using a different synthetic procedure. In this case, solid ZnI_2 (0.349 mmol, 0.1114 g) was added to a solution of **4-pn** (0.704 mmol, 0.2030 g) in 10 ml DMF. The resulting solution was stirred for about fifteen to twenty minutes and was then left uncovered at room temperature for crystallization. Slow evaporation of the DMF solvent resulted in the formation of white, plate-like crystals of **4-pnZnI** (0.1671 g) after two to three weeks. A yield of 53% was obtained.

Elemental analysis for $[Zn(C_{18}H_{12}N_2O_2)_2I_2]$, (**4-pnZnI**) (%): **Calcd.**: C, 48.27; H, 2.70; N, 6.25: **Found**: C, 48.59; H, 2.59; N, 6.35.

Instrumental studies

Single crystal X-ray diffraction

A Rigaku XtaLAB Synergy R single crystal X-ray diffractometer was employed for the collection of diffraction data for structures **4-pnZnI**, **4-pnCoCl** and **4-pnCoBr**. The instrument was equipped with a HyPix CCD detector, and a rotating anode X-ray source. Cooling to 150(2) K was achieved by an Oxford Cryogenics Cryostat, and data were collected *via* ω scans. CuK-α radiation ($\lambda = 1.54184$ Å) was employed for structures **4-pnCoCl** and **4-pnZnI**, and MoK-α radiation ($\lambda = 0.71073$ Å) was used for structure **4-pnCoBr**. The software program CrysAlisPro (Version 1.171.40.23a) [19] was used for data reduction and absorption corrections.

A Bruker D8 Venture single crystal X-ray diffractometer, equipped with a Photon 100 CMOS detector, was employed to collect diffraction data for structures **4-pnHgI** and **4-pnZnBr**. Data were collected at 150(2) K, using ϕ and ω scans. The crystals were irradiated with MoK-α radiation ($\lambda = 0.71073$ Å), and cooled using an Oxford Cryogenics Cryostat. The program SAINT+ [20] was employed for data reduction, and SADABS [21] for absorption corrections. Both these programs form part of the APEX II [22] suite of programs.

The crystal structures were solved *via* direct methods or intrinsic phasing using SHELX-2013 [23], as part of WinGX [24], while the structures were refined using SHELXL [25], as part WinGX [24]. For all the structures, the hydrogen atoms were placed in calculated positions riding on their parent atoms. The software Mercury [26] and Platon [27] were used to generate figures analyze the structures.

Powder X-ray diffraction

Samples for powder X-ray diffraction were prepared by sprinkling the powder sample on a low-back ground silicon sample holder. Powder X-ray diffraction patterns were collected on a Bruker D2 Phaser instrument, at room temperature. The software DiffractWD [28] was used to compare the experimental powder patterns with powder patterns calculated from single crystal data. These comparisons are given in Supplementary Information Section 1.

Table 1. Synthetic information for the synthesis of the coordination complexes 4-pnCoCl, 4-pnCoBr, 4-pnZnBr and 4-pnHgI.

	Mass **4-pn** (g)	Mass MX_2 (g)	Crystal Description	Product Mass (g)	Yield (%)	Elemental Analysis
4-pnCoCl	0.2005 (0.695 mmol)	$MX_2 = CoCl_2$ 0.0452 (0.348 mmol)	Purple, fluff-like crystals	0.0786	32	$[Co(C_{18}H_{12}N_2O_2)_2Cl_2]$, **Found**: C, 61.53; H, 3.05; N, 8.26. **Calcd.**: C, 61.21; H, 3.42; N, 7.93
4-pnCoBr	0.2016 (0.699 mmol)	$MX_2 = CoBr_2$ 0.0770 (0.352 mmol)	Blue, plate-like crystals	0.1140	41	$[Co(C_{18}H_{12}N_2O_2)_2Br_2]$, **Found**: C, 54.39; H, 2.90; N, 6.89. **Calcd.**: C, 54.37; H, 3.04; N, 7.04
4-pnZnBr	0.2031 (0.704 mmol)	$MX_2 = ZnBr_2$ 0.0789 (0.350 mmol)	White, plate-like crystals	0.1129	40	$[Zn(C_{18}H_{12}N_2O_2)_2Br_2]$, **Found**: C, 53.97; H, 2.72; N, 7.02. **Calcd.**: C, 53.93; H, 3.02; N, 6.99
4-pnHgI	0.2026 (0.703 mmol)	$MX_2 = HgI_2$ 0.1597 (0.351 mmol)	Orange-yellow plate-like crystals	0.0978	27	$[Hg(C_{18}H_{12}N_2O_2)_2I_2]$, **Found**: C, 41.68; H, 1.92; N, 5.63. **Calcd.**: C, 41.94; H, 2.35; N, 5.43

Solid-state fluorescence spectra

Samples for the measurement of fluorescence spectra were prepared by sandwiching a thin layer of the compound to be analyzed between two glass microscope slides. A Horiba Fluoromax-4 spectrofluorometer was used to collect solid-state fluorescence spectra at room temperature. The instrument was equipped with a photomultiplier detector, a xenon lamp light source and a plane-grating Czerny-Turner spectrometer. The wavelength range of the optical system was 200 nm to 950 nm, and for both excitation and emission spectra, a front entrance and exit slit of 5.00 nm band pass was used. The samples were measured at a 45° geometry.

Results

Crystallographic discussion of structures

Five new crystal structures that combine the organic ligand **4-pn** with divalent metal halides ZnX_2 ($X = Br^-$ or I^-), CoX_2 ($X = Cl^-$ or Br^-) or HgI_2, were obtained, with the line structures of the complexes shown in Scheme 2. The structures will be abbreviated as **4-pnMX**, with **4-pn** indicating the organic ligand, **M** the metal ion, and **X** the halido ligand.

Three different types of structures were obtained. Structure **4-pnZnBr** was found to be isostructural to structures **4-pnCoBr** and **4-pnZnI**. All the structures display isolated, zero-dimensional coordination complexes, of the formula $[M(4\text{-pn})_{2\times 2}]$, with the metal centers coordinated to two halido and two organic ligands *via* the aromatic nitrogen atom and displaying a distorted tetrahedral geometry. The crystallographic parameters of these structures are listed in Table 2 and the molecular structures of the complexes are illustrated in Figure 1. Selected bond lengths, angles, torsion angles and other geometric parameters are listed in Table S2.1 in the Supplementary Information Section 2.

Structure 4-pnCoCl

Structure **4-pnCoCl** crystallizes in the space group *Fdd*2 and its asymmetric unit comprises half a Co(II) metal center, coordinated to one chlorido ligand and one **4-pn** ligand, *via* the nitrogen atom of the N-donor **4-pn** ligand, as shown in Figure S3.1 in the Supplementary Information Section 3. The Co(II) ion is located on a two-fold rotation axis, which generates the second half of the $[Co(4\text{-pn})_2Cl_2]$ complex molecule, which is shown in Figure 1. In the molecule, the Co(II) center adopts a four-coordinated,

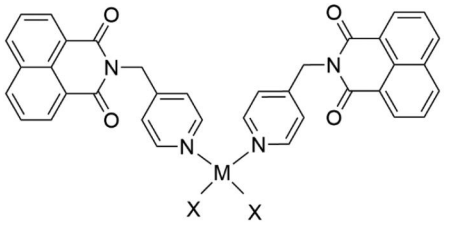

4-pnCoCl: L=**4-pn**, $MX_2 = CoCl_2$
4-pnCoBr: L=**4-pn**, $MX_2 = CoBr_2$
4-pnZnBr: L=**4-pn**, $MX_2 = ZnBr_2$
4-pnZnI: L=**4-pn**, $MX_2 = ZnI_2$
4-pnHgI: L=**4-pn**, $MX_2 = HgI_2$

Scheme 2. Structures reported in this study.

Table 2. Crystallographic parameters and refinement results for the 4-pnMX structures.

Structure	4-pnCoCl	4-pnCoBr	4-pnZnBr	4-pnZnI	4-pnHgI
Empirical formula	$[Co(C_{18}H_{12}N_2O_2)_2Cl_2]$	$[CoBr_2(C_{18}H_{12}N_2O_2)_2]$	$[ZnBr_2(C_{18}H_{12}N_2O_2)_2]$	$[Zn(C_{18}H_{12}N_2O_2)_2I_2]$	$[Hg(C_{18}H_{12}N_2O_2)_2I_2]$
Formula weight/g.mol^{-1}	706.42	795.32	801.78	895.78	1030.98
Temperature/K	150(2)	150(2)	150(2)	150(2)	150(2)
Wavelength/Å	1.54184	0.71073	0.71073	1.54184	0.71073
Crystal system	Orthorhombic	Orthorhombic	Orthorhombic	Orthorhombic	Monoclinic
Space group	*Fdd*2	*Pbcn*	*Pbcn*	*Pbcn*	*C2/c*
Unit cell dimensions					
a/Å	53.292(3)	27.0179(8)	27.003(3)	27.7689(3)	28.180(2)
b/Å	25.1269(14)	7.2177(3)	7.2208(8)	7.26850(10)	4.7604(3)
c/Å	4.3407(3)	15.7647(5)	15.7711(19)	15.8408(2)	49.173(4)
α/°	90	90	90	90	90
β/°	90	90	90	90	106.303(2)
γ/°	90	90	90	90	90
Volume/Å^3	5812.5(6)	3074.23(18)	3075.1(6)	3197.28(7)	6331.2(8)
Z	8	4	4	4	8
Density (calculated)/Mg/m^3	1.615	1.718	1.732	1.861	2.163
Absorption coefficient/mm^{-1}	6.750	3.207	3.447	16.620	6.861
F(000)	2888	1588	1600	1744	3888
Crystal size/mm^3	$0.005 \times 0.008 \times 0.068$	$0.037 \times 0.048 \times 0.140$	$0.120 \times 0.335 \times 0.388$	$0.034 \times 0.078 \times 0.175$	$0.031 \times 0.043 \times 0.245$
Theta range for data collection/°	3.3160 − 72.5020	1.507 to 29.910	2.583 to 24.711	3.183 to 78.655	2.589 to 26.382
Reflections collected	15304	39063	69626	23036	84898
Independent reflections	2575 [R(int)= 0.0816]	4066 [R(int)= 0.1386]	2635 [R(int) = 0.0517]	3328 [R(int) = 0.0731]	6434 [R(int) = 0.0438]
Completeness to θ (%)	100	100	94.2	100	99.9
Max. and min. transmission	1.000 and 0.416	1.000 and 0.245	0.745 and 0.439	1.000 and 0.048	0.745 and 0. 557
Data/restraints/ parameters	2575/1/213	4066/0/213	2635/0/213	3328/0/213	6434/0/424
Goodness-of-fit on F^2	1.091	1.040	1.078	1.187	1.103
Final *R* indices [$I > 2\sigma(I)$]	R1 = 0.0430, wR2 = 0.0994	R1 = 0.0462, wR2 = 0.0986	R1 = 0.0236, wR2 = 0.0630	R1 = 0.0460, wR2 = 0.1525	R1 = 0.0240, wR2 = 0.0482
R indices (all data)	R1 = 0.0667, wR2 = 0.1177	R1 = 0.0757, wR2 = 0.1084	R1 = 0.0252, wR2 = 0.0641	R1 = 0.0468, wR2 = 0.1530	R1 = 0.0281, wR2 = 0.0492
Largest diff. peak and hole/e.Å^{-3}	0.418 and −0.485	0.576 and −0.714	0.311 and −0.459	2.194 and −1.689	0.902 and −0.553

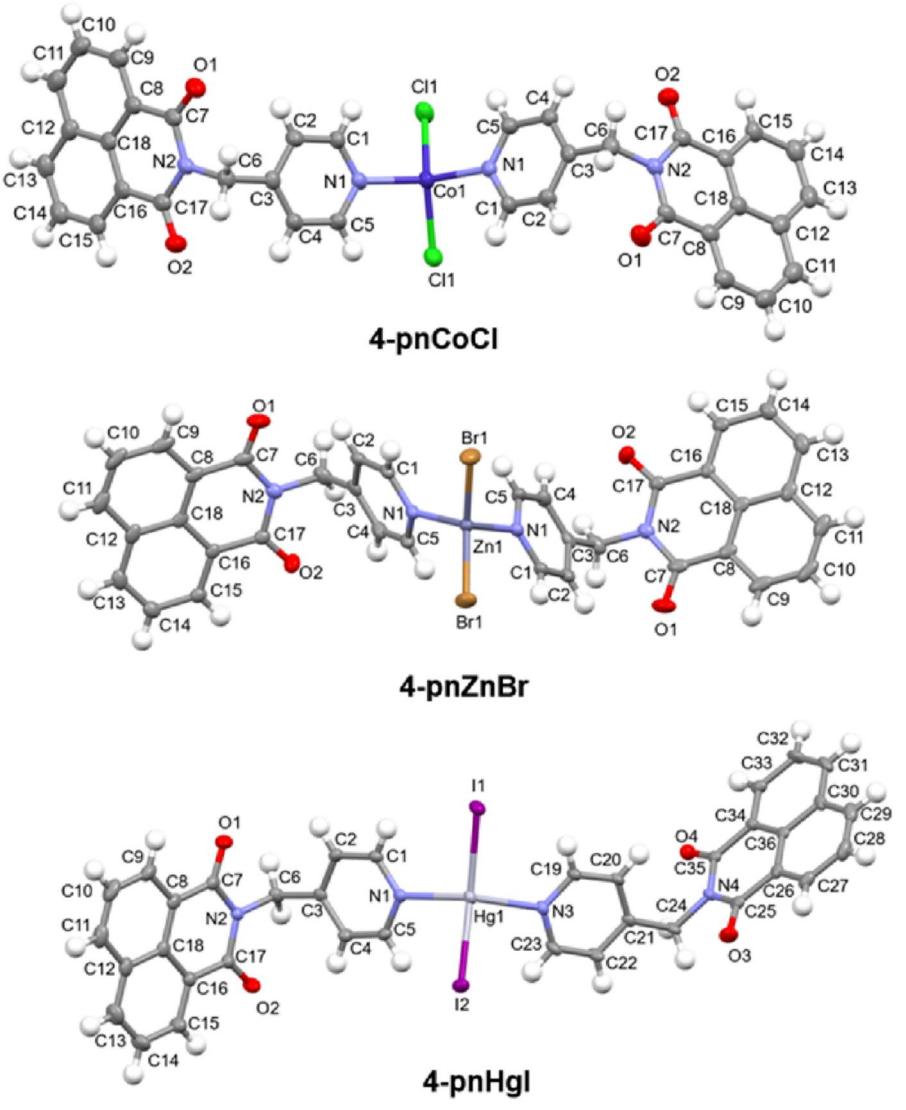

Figure 1. Molecular structures of the coordination complexes **4-pnCoCl, 4-pnZnBr** (also a representative of the molecular structures of the isostructural structures **4-pnCoBr** and **4-pnZnI)** and **4-pnHgI**, illustrating the atomic numbering scheme. Ellipsoids are drawn at the 50% probability level.

distorted tetrahedral geometry, illustrated in Figure 2(a), with a Co-N bond length of 2.063(4) Å and a Co-Cl bond length of 2.2547(14) Å. The N-Co-Cl angles fall within the range 99.82(12)° to 102.20(12)° while the N-Co-N angle is 125.1(3)° and the Cl-Co-Cl angle is 131.02(10)°, indicating the distortion from the ideal tetrahedral geometry. Due to the fact that the Co(II) ion is located on a two-fold rotation axis, the two **4-pn** ligands adopt the same conformation, with a N(2)-C(6)-C(3) angle of 111.9(5)° at the methylene group connecting the rigid naphthalimide portion to the pyridyl group.

The molecules pack along the *a*-axis forming perpendicular stacks, with aromatic interactions between the 1,8-naphthalimide groups and pyridine groups, as illustrated

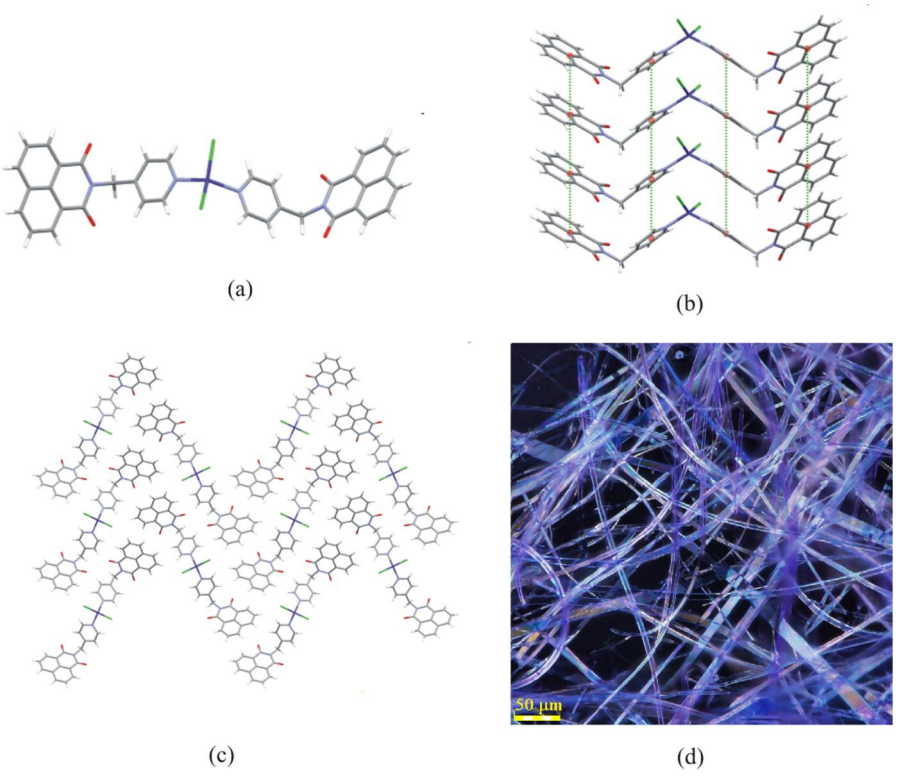

Figure 2. (a) Conformation of complex in **4-pnCoCl**. (b) Aromatic interactions in stack. (c) Packing of **4-pnCoCl** when viewed down the *c*-axis. (d) Crystalline fibers of **4-pnCoCl**, showing curved fibers.

in Figure 2(b). The centroid-to-centroid distance between the aromatic moieties is 4.341 Å. Figure 2(c) shows the packing diagram of structure **4-pnCoCl**, viewed down the *c*-axis, showing that the molecules pack to form a V-shaped, herringbone packing.

The crystal habit of the complex **4-pnCoCl** proved to be very interesting since it formed very fine, long fibers upon crystallization, with diameters of 5 to 10 μm, as shown in Figure 2(d), with some fibers being curved. Reddy *et al.* [29] investigated the bending of organic crystals, and found that crystals in which intermolecular interactions in different directions differ in strength, may exhibit bending. These often include compounds containing aromatic stacks similar to what is observed in the structure of **4-pnCoCl**.

Structures 4-pnCoBr, 4-pnZnBr and 4-pnZnI

Structures **4-pnCoBr**, **4-pnZnBr** and **4-pnZnI** are isostructural, crystallizing in space group *Pbcn*, and they will be discussed together. The asymmetric unit of these structures contains half a metal ion coordinated to one halido ion and one **4-pn** ligand, as illustrated in Figure S3.1 in the Supplementary Information Section 3. The metal ion is located on a two-fold rotation axis, with the rest of the $[M(4\text{-pn})_2\times_2]$ complex generated by this symmetry operator, with the full complex molecule shown in Figure 1.

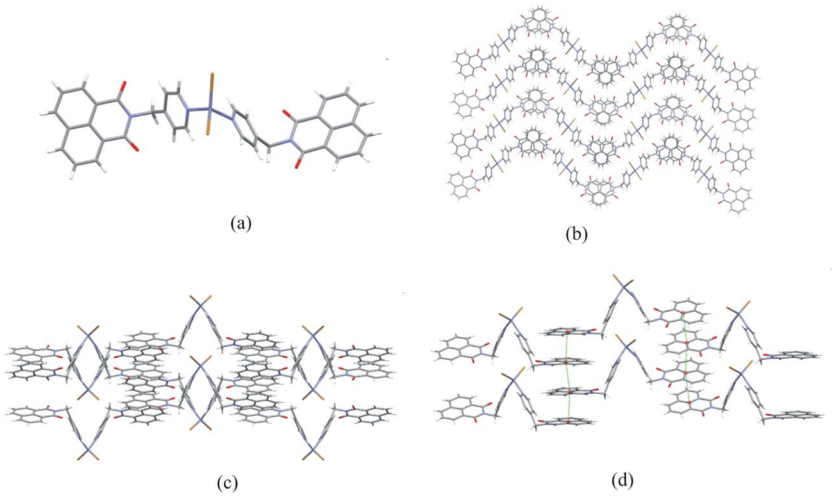

Figure 3. (a) Complex molecule in **4-pnZnBr**. (b) Packing of **4-pnZnBr** viewed down the *b*-axis. (c) Packing of **4-pnZnBr** viewed down the *c*-axis. (d) Aromatic interactions in **4-pnZnBr**. Structure **4-pnZnBr** is also representative of structures **4-pnZnI** and **4-pnCoBr**.

In these three complexes, the metal cation is coordinated in a distorted tetrahedral geometry, as shown in Figure 3(a), by two halido anions, with a X-M bond length of 2.3552(3) Å in **4-pnZnBr**, 2.5488(5) Å in **4-pnZnI** and 2.3715(4) Å in **4-pnCoBr**, indicating that an increase in size of halido ligand brings about an increase in M-X bond length. The metal cation is also coordinated to two **4-pn** organic ligands, with a Zn-N bond length of 2.0659(18) Å in **4-pnZnBr**, 2.066(4) Å in **4-pnZnI** and a Co-N bond length of 2.046(2) Å in **4-pnCoBr**, indicating the bigger size of the zinc ion compared to the cobalt ion.

The distortion from the ideal tetrahedral geometry around the metal centers is evident from the angles involving the metal ion. The N-M-N and X-M-X angles are 93.80(10)° and 121.02(2)° in **4-pnZnBr,** 93.8(2)° and 119.17(4)° in **4-pnZnI** and 95.91(14)° and 117.87(3) in **4-pnCoBr**. The N-M-X angle ranges from 104.30(5)° to 115.20(5)° in **4-pnZnBr,** 106.08(10)° to 114.50(10)° in **4-pnZnI** and from 104.36(6)° to 116.31(6)° in **4-pnCoBr**. Due to the symmetry of the molecule, the two **4-pn** organic ligands adopt the same conformation.

Figure 3(b) and (c) illustrate the packing of complex molecules in structure **4-pnZnBr**. When viewed along the *b*-direction, the molecules pack with the 1,8-naphtalimide groups of neighboring molecules forming a stack, as shown in Figure 3(b). A layered structure is formed, with the 1,8-naphthalimide groups forming a layer, and the metal halide and pyridyl groups packing in a second layer, as shown in Figure 3(b) and 3(c). Figure 3(b) reveals that the coordination complexes pack in a zig-zag manner. Viewed down the *b*-axis, aromatic interactions zipper neighbouring molecules together, resulting in a highly ordered molecular assembly as can be seen in Figure 3(b), with parallel aromatic ring planes. The perpendicular distance between the parallel organic moieties is 3.622 Å in **4-pnZnBr**, 3.646 Å in **4-pnZnI**, and 3.619 Å in **4-pnCoBr** indicating the presence of aromatic interactions between the aromatic groups, as shown in Figure 3(d).

Structure 4-pnHgI

Structure **4-pnHgI** crystallizes in the monoclinic space group *C*2/*c*, with the complex molecule comprising one Hg(II) ion, to which two N-donor organic **4-pn** ligands and two iodido ligands are coordinated, as illustrated in Figure 1. The **4-pn** ligand containing atom N(1) will be referred to as organic ligand 1, and the **4-pn** ligand containing atom N(3) will be denoted as organic ligand 2.

As shown in Figure 4(a), the complex displays a distorted tetrahedral geometry, with Hg-I bond lengths of 2.6762(3) Å and 2.6942(3) Å, and two Hg-N bond lengths of 2.410(3) Å. These bond lengths are longer than the corresponding bonds in structures **4-pnZnBr**, **4-pnZnI**, **4-pnCoCl** and **4-pnCoBr** due to the larger Hg(II) ion and larger I^- ions.

The coordination geometry around the metal ion is distorted from an ideal tetrahedral geometry, as shown in Figure 4(a), with N-Hg-I angles ranging from 95.68(7)° to 100.15(7)°. The N-Hg-N and I-Hg-I angles have values of 118.76(10)° and 148.351(10)° respectively. As a result of the two halves of the complex not being symmetry related, the two 1,8-naphthalimide groups of the organic ligands do not display the same orientation relative to the pyridyl group, with the 1,8-naphthalimide group in ligand 2 being more rotated relative to the plane of the pyridyl group compared with that in ligand 1. The angle between the plane of the 1,8-naphthalimide group and the plane of the pyridyl moiety connected to this group is 71.55° in ligand 1, whereas the corresponding angle in ligand 2 is 83.45°. The difference in the conformations of the **4-pn** ligands, ligand 1 and ligand 2, is illustrated in Figure 4(b).

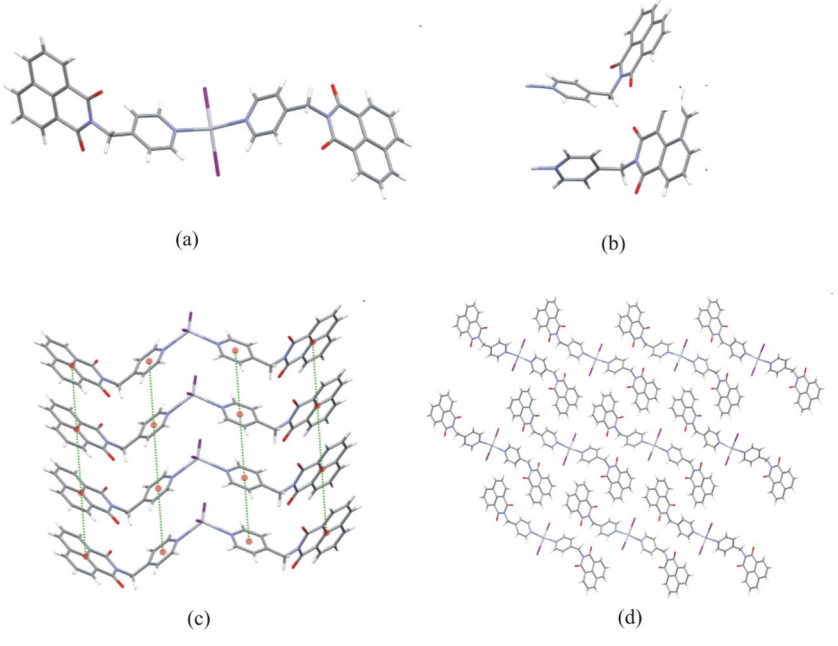

Figure 4. (a) Complex molecules in **4-pnHgI**. (b) Different **4-pn** ligand conformations. Ligand 1 (top), ligand 2 (bottom). (c) Long centroid-to-centroid distances between the aromatic groups. (d) Packing of **4-pnHgI** viewed down the *b*-axis.

The complex molecules stack in the *b*-direction, as illustrated in Figure 4(c), with centroid-to-centroid distances in the stack equal to 4.760 Å, a distance which is too long for aromatic interactions. The packing diagram of **4-pnHgI**, viewed along the *b*-axis, is shown in Figure 4(d), indicating a layered type packing, with the HgI_2 portion of the complex molecule forming the inorganic layer, and the **4-pn** ligand the organic layer.

Discussion of 4-pnMX structures

The five new crystal structures all contain complexes of the molecular formula [M(4-pn)$_2\times_2$], however, three different structural types are formed by the members of the series. The structure formed can be correlated with the sum of the ionic radii of the metal ion and halido ligand. In the case of structure **4-pnCoCl**, both the metal ion and halido ligand are small, with a combined sum of radii of 2.39 Å, and the structure crystallizes in the space group *Fdd2*. For the isostructural structures **4-pnCoBr**, **4-pnZnBr** and **4-pnZnI**, the sum of ionic radii equal 2.54 Å, 2.56 Å and 2.80 Å respectively, and these structures crystallize in space group *Pbcn*. Lastly, when the large Hg(II) ion and iodido ligand are combined with the **4-pn** ligand in structure **4-pnHgI**, the sum of ionic radii of the metal ion and halido ligand is 3.16 Å, and the structure crystallizes in space group *C*2/*c*.

The conformations of the [M(4-pn)$_2\times_2$] complexes are compared in Figure 5. Even though the same general conformation is exhibited, clear differences between the conformations of the complexes are evident. The complexes in **4-pnCoBr**, **4-pnZnBr**, **4-pnZnI** and **4-pnCoCl** are symmetric, but this is not the case for **4-pnHgI**. A distorted tetrahedral geometry is displayed by all the metal centers, but with different degrees of distortion. The complex **4-pnHgI** shows a high degree of distortion, with a I-Hg-I angle of 148.351(11) Å since this larger angle ensures less steric hindrance between the two large iodido ligands.

Because of the different conformations adopted by the complexes, different packing arrangements are exhibited, however, aromatic interactions play a prominent role in the packing of all the complexes. Only weak CH … O and CH … X hydrogen bonding interactions are present in all the complexes.

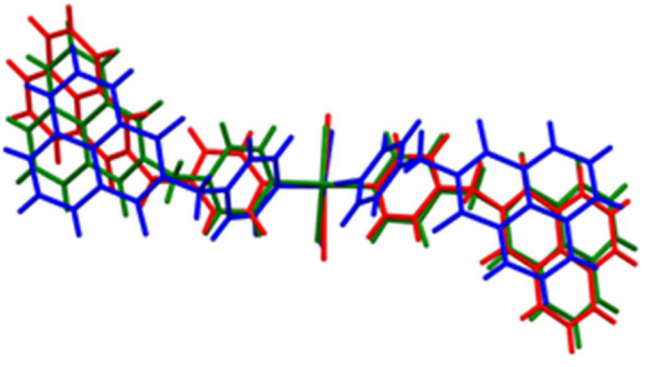

Figure 5. Overlay of complex molecules. **4-pnCoCl**: green, **4-pnZnBr**: blue (representative of **4-pnCoBr and 4-pnZnI**), **4-pnHgI**: red.

It is interesting to note that, unlike the coordination complexes obtained from the combination of the related ((3-pyridyl)methyl)-1,8-naphthalimide ligand with divalent metal halides, which were found to all incorporate solvent molecules into their crystal structures [17], none of the structures of the **4-pn** containing complexes incorporated solvent molecules, despite the fact that the two organic ligands only differ in the position of the nitrogen atom on the pyridine ring by one.

Solid-state fluorescence studies

The solid-state fluorescence spectra of the organic ligand **4-pn** and the **4-pnMX** complexes under investigation were studied. Table 3 lists the optimized excitation wavelength for each complex as well as the emission wavelength(s). The fluorescence spectra are shown in Figure 6.

As shown in Figure 6, the organic ligand, **4-pn**, exhibits a broad emission band at 450 nm due to its structural rigidity and conjugated π-system, allowing for an efficient π-π* transition [30]. When coordinated to a metal halide, charge transfer interactions may occur between the organic ligand and the metal halide in the coordination complex, resulting in a shift of the emission maximum relative to the uncoordinated

Table 3. Fluorescence excitation and emission wavelengths for the ligand, 4-pn, and 4-pnMX complexes.

Compound	Fluorescence excitation wavelength (nm)	Fluorescence emission wavelength(nm)	Shift of emission maximum from 4-pn ligand (nm)
4-pn	371	450	–
4-pnCoCl	335	418	32 (Blue shift)
4-pnCoBr	350	410	40 (Blue shift)
4-pnZnBr	368	454	4 (Red shift)
4-pnHgI	347	426	24 (Blue shift)
4-pnZnI	371	446, 419	4, 31 (Blue shift)

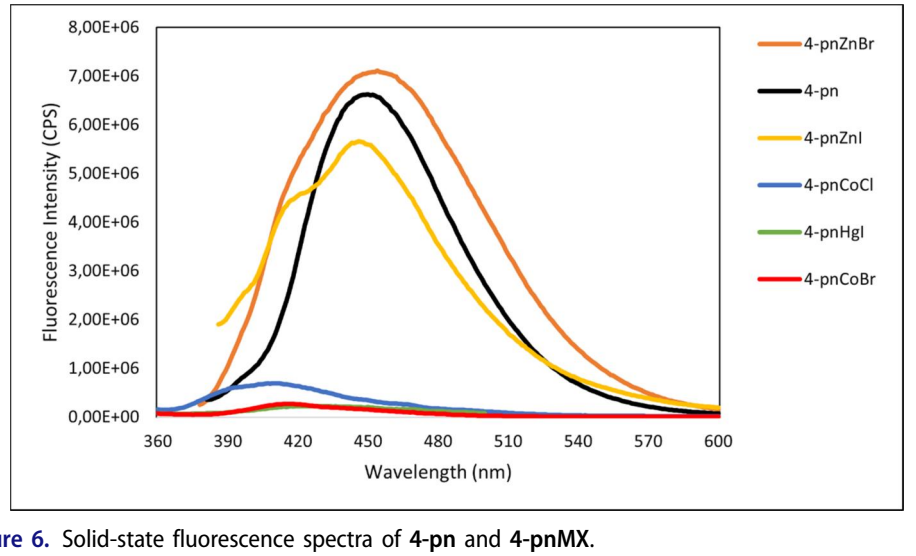

Figure 6. Solid-state fluorescence spectra of **4-pn** and **4-pnMX**.

ligand [31]. The identity of the coordinated metal ion and the halido ligand may also cause fluorescence quenching or enhancement.

Metal-to-ligand charge-transfer and ligand-to-metal charge-transfer transitions also influence the emission intensities in coordination complexes [32]. Complexes that contain "lighter" diamagnetic metal ions have been found to cause fluorescence enhancement relative to the free ligand while complexes that have heavier diamagnetic ions result in fluorescence quenching, due to the heavy-atom effect [18,32]. Furthermore, complexes with paramagnetic ions show substantial quenching as compared to the free ligand [18,32]. The nature of the halide ion also affects the fluorescence intensity of the complex due to the heavy ion effect [33], with a bromide anion quenching more than a chloride anion [34–36].

The fluorescence enhancement observed in the Zn(II) complex, **4-pnZnBr**, compared to the parent ligand, **4-pn**, seen in Figure 6, can be attributed to the presence of the diamagnetic Zn(II) ion causing extra rigidity in the complex, reducing the non-radiative pathways and hence suppressing the loss of energy [37]. The fluorescence quenching observed for the Co(II) complexes, **4-pnCoCl** and **4-pnCoBr**, compared to the parent ligand, **4-pn**, observed in Figure 6, is due to the paramagnetic Co(II) ion in the complex. Upon excitation, ligand-to-metal-charge-transfer occurs, resulting in non-radiative deactivation, hence quenching is observed [38]. The paramagnetic ion enhances inter-system crossing (from the singlet excited state to the triplet excited state) leading to phosphorescence or non-radiative deactivation, hence fluorescence quenching occurs [34]. The quenching of the emission of **4-pnZnI** and **4-pnHgI** can be explained by the heavy ion effect, with the introduction of the iodide anion in both complexes and the mercury metal centre in the latter [39]. The complex **4-pnZnI** displays lower intensity than **4-pnZnBr** and **4-pnCoBr** displays more quenching than **4-pnCoCl** due to the heavier iodido ligand compared to the bromido ligand and the heavier bromido ligand compared to the lighter chlorido ligand respectively [33,36,40].

Complexes **4-pnZnBr** and **4-pnZnI** show emission maxima at a similar wavelengths to the **4-pn** ligand, at 454 nm and 446 nm respectively, indicating that the fluorescence arises purely from the π-π^* transition within the ligand [41]. Complex **4-pnZnI**, however, exhibits an additional, lower intensity emission peak superimposed on the main fluorescence peak, at 419 nm, as can be seen in Figure 6, indicating dual fluorescence emission for this complex. Based on the shape of the emission peak of complex **4-pnZnBr**, this second fluorescence peak may also be present for this compound, however, is most likely hidden by the main fluorescence peak 454 nm. It has been reported in the literature that the 4-pn ligand exhibits dual fluorescence [12]. The wavelength of the second peak observed for complex **4-pnZnI** is similar to the emission wavelengths of the complexes **4-pnCoCl**, **4-pnCoBr** and **4-pnHgI** which are blue-shifted relative to the emission peak of the parent ligand, **4-pn**.These complexes emit at 418 nm, 410 nm and 426 nm respectively. The shift of emission to lower wavelengths for **4-pnCoCl**, **4-pnCoBr** and **4-pnHgI** may be attributed to intermolecular charge transfer between the metal ion and the organic ligand [31].

The solid-state fluorescence of the **4-pnMX** complexes reported here may be compared to the solid-state fluorescence reported for the family of ionic compounds comprised of *N*-(4-picolinium)-1,8-naphthalimide cations and tetrahalometallate anions

reported previously [16]. In these ionic compounds, the *N*-(4-picolinium)-1,8-naphthalimide cation is the protonated version of the **4-pn** molecule, and will be abbreviated **4-pnH**, with the tetrahalometallate ($[MX_4]^{2-}$) anions acting as counter ions. These ionic compounds will be abbreviated **4-pnHMX**, where M is the metal ion and X the halido ligand. In addition, this study also reported the fluorescence of **4-pn** molecule. The study found that the fluorescence of the ionic compounds **4-pnHCoCl** and **4-pnHCoBr** was completely quenched due to the presence of the paramagnetic ion. Fluorescence quenching, albeit not complete quenching, was also observed for the **4-pnCoCl** and **4-pnCoBr** complexes in the current study. The emission intensities of both the **4-pnCoCl** and **4-pnCoBr** complexes studied in the current investigation were higher compared to the related ionic compounds **4-pnHCoCl** and **4-pnHCoBr**, reported in the literature, showing a higher emission intensity from the complexes compared to the ionic compounds.

The **4-pnHZnCl** and **4-pnHCdCl** ionic compounds showed emission enhancement relative to the **4-pn** molecule, whereas the **4-pnHHgCl** and **4-pnHZnBr** ionic compounds exhibited fluorescence quenching relative to that of **4-pn**, but still showed significant fluorescence emission [16]. In the current study, the **4-pnZnBr** complex showed emission enhancement relative to **4-pn**. This means that the ionic compound **4-pnHZnBr** [16] showed a lower emission intensity than the complex **4-pnZnBr** studied in the current investigation, indicating that in this case, again, the coordination complex exhibits higher fluorescence intensity than the related ionic compound. This observation may be explained by the coordination complexes adopting stronger electronic coupling between the metal center and the organic ligand, as well as enhanced structural rigidity, compared to the ionic compounds, thus enhancing fluorescence emission.

The fluorescence wavelengths of the compounds **4-pnHZnCl**, **4-pnHCdCl**, **4-pnHHgCl** and **4pnHZnBr** ranged from 451 nm to 458 nm, and were all clustered around that of the **4-pn** molecule at 454 nm, which is similar to what is observed for the **4-pnZnBr** and **4-pnZnI** complexes in the current study, with respective emission wavelengths of 454 nm and to 446 nm. The emission wavelength of complex **4-pnZnBr**, which emits at 454 nm, and the emission wavelength of the ionic compound **4-pnHZnBr**, which emits at 458 nm, is similar, which indicates that both the ionic compound and the complex containing the same metal halide component, emit at similar wavelengths. In addition, comparison of the fluorescence results of the current study and the literature study indicate that in the case of the compounds containing diamagnetic metal ions, both the ionic and coordination compounds emit at wavelengths similar to that of the **4-pn** molecule, indicating that the π-π^* transition of the **4-pn** fluorophore dominates the emission process.

Conclusions

The fluorophore, N-((4-pyridyl)methyl)-1,8-naphthalimide, **4-pn**, was successfully synthesized, and incorporated into coordination complexes through the reaction with metal halides. Five coordination complexes, of the formula $[M(C_{18}H_{12}N_2O_2)_2\times_2]$,

containing **4-pn** and different metal halide components, were structurally characterized and their solid-state fluorescence investigated.

Even though all the complex molecules show similar geometries, three different structure types were observed, and it was found that the specific crystal structure formed correlated with the sum of the ionic radii of the metal ion and halido ligand. Of specific interest was the crystal habit of compound **4-pnCoCl**, which crystallizes to form long, flexible and bendable fibers.

It was also found that the coordination of the organic ligand to a diamagnetic metal, such as a Zn(II) ion may cause fluorescence enhancement relative to the parent ligand, **4-pn**, while the coordination of the organic ligand to heavy metal ions (e.g. Hg(II)) or paramagnetic ions (e.g. Co(II)) resulted in significant quenching of fluorescence emission. The nature of the halido ligand coordinated to the metal centre also has an effect on the fluorescence intensity of the complex, with the iodido ligand quenching the fluorescence emission more than the bromido ligand and the bromido ligand, in turn, quenching more than the chlorido ligand. Thus, the fluorescence intensity and wavelength of the complexes are influenced by the identity of the metal ion and halido ligand comprising the complex. The identification of these trends allows for the tweaking of the emission wavelength and intensity of the complexes.

Compared to the ionic compounds prepared from **4-pn** and metal halides, it was found that the associated coordination complexes investigated in the current study exhibit higher fluorescence intensities than the corresponding ionic compounds reported in literature [16]. This important observation is ascribed to the increased rigidity and stronger electronic coupling present in the coordination complexes.

The improved solid-state fluorescence of the coordination complexes, compared to their ionic counterparts, spot them as potential candidates to a wide range of applications. The tunable fluorescence suggests that naphthalimide ligands, like **4-pn**, are responsive when coordinated to metal halides and they may have potential applications in metal ion detection and anion sensing. Specifically, as found in this study, **4-pn** shows strong fluorescence upon coordination with Zn(II) halides, indicating its potential for use as a sensor for these species. Future work will be conducted on the stability of these complexes for practical applications.

CCDC 2430030–2430034 contains the supplementary crystallographic data for structures. These data can be obtained free of charge *via* http://www.ccdc.cam.ac.uk/conts/retrieving.html, or from the Cambridge Crystallographic Data Centre, 12 Union Road, Cambridge CB2 1EZ, UK; fax: (+44) 1223–336-033; or e-mail: deposit@ccdc.cam.ac.uk.

CRediT authorship contribution statement

B.M.P Beebeejaun-Boodoo: Synthesis, Structural analysis, Fluorescence studies, Writing and editing of manuscript.

Melanie Rademeyer: Structural analysis, Conceptualization, Funding acquisition, Editing of manuscript.

Acknowledgements

The authors would like to thank Frikkie Malan for assistance with crystallographic aspects.

Author contributions

CRediT: **B. M. Parveen Beebeejaun-Boodoo**: Data curation, Investigation, Methodology, Validation, Visualization, Writing – original draft, Writing – review & editing; **Melanie Rademeyer**: Conceptualization, Funding acquisition, Project administration, Writing – review & editing.

Disclosure statement

No potential conflict of interest was reported by the author(s).

Funding

This work was supported by the National Research Foundation, South Africa under [Grant No: SRUG210427597644] and the University of Pretoria as part of the RDP programme.

References

[1] A.K. Srivastava, A. Singh, L. Mishra. *J. Phys. Chem. A*, **120**, 4490 (2016).
[2] S. Thavornpradit, J. Sirirak, N. Wanichacheva. *J. Photochem. Photobiol. A: Chem*, **330**, 55 (2016).
[3] J.-A. Gan, Q.L. Song, X.Y. Hou, K. Chen, H. Tian. *J. Photochem. Photobiol. A: Chem*, **162**, 399 (2004).
[4] (a) M.D. McGehee, A.J. Heeger. *Adv. Mater.*, **12**, 1655–1668 (2000);(b) V. Bojinov, I. Grabchev. *Dyes Pigm.*, **51**, 57 (2001).
[5] Y.Q. Gao, R.A. Marcus. *J. Phys. Chem. A*, **106**, 1956 (2002).
[6] (a) S. Kagatikar, D. Sunil. *J. Mater. Sci.*, **57**, 105 (2022);(b) R.-F. Jin, S.-S. Tang, W.-D. Sun. *Tetrahedron*, **70**, 47 (2014).
[7] X. Cao, L. Meng, Z. Li, Y. Mao, H. Lan, L. Chen, Y. Fan, T. Yi. *Langmuir*, **30**, 11753 (2014).
[8] H. Yu, Y. Guo, W. Zhu, K. Havener, X. Zheng. *Coord. Chem. Rev*, **44**, 214019 (2021).
[9] I.K. Grabtschev, I.T. Moneva, E. Wolarz, D. Bauman. *Sect. A: J. Phys. Sci*, **51**, 1185 (1996).
[10] E. Martin, R. Weigand, A. Pardo. *J. Lumin*, **68**, 157 (1996).
[11] R.J. Sarma, C. Tamuly, M.N. Barooah, J.B. Baruah. *J. Mol. Struct*, **829**, 29 (2007).
[12] (a) J.K. Nath, J.B. Baruah. *J. Fluoresc.*, **24** (3), 649 (2014);(b) K. Ramasamy, S. Thambusamy, *Sensors and Actuators B: Chem.*, **247**, 632 (2017); (c) S. Paudel, P. Nandhikonda, M.D. Heagy. *J. Fluoresc.*, **19** (4), 681 (2009); (d) P. Nandhikonda, M.D. Heagy. *Org. Lett.*, **12** (21), 4796 (2010).
[13] A. Demeter, T. Bérces, L. Biczók, V. Wintgens, P. Valat, J. Kossanyi. *J. Phys. Chem.*, **100**, 2001 (1996).
[14] H. Cao, V. Chang, R. Hernandez, M.D. Heagy. *J. Org. Chem.*, **70**, 4929 (2005).
[15] F.R. Allen. *Acta Crystallogr, Sect. B: Struct. Sci.*, **58**, 380 (2002).
[16] B.M.P. Beebeejaun-Boodoo, R. Erasmus, M. Rademeyer. *CrystEngComm.*, **20**, 4875 (2018).
[17] B.M.P. Beebeejaun-Boodoo, M. Rademeyer. *Pure Appl. Chem.*, **95**, 273 (2023).
[18] See, among others:(a) D.S. McClure. *J. Chem. Phys.*, **20**, 682 (1952); (b) T.L. Banfield, D. Husain. *Trans. Faraday Soc.*, **65**, 1985 (1969); (c) A.W. Varnes, R.B. Dodson, E.L. Wehry. *J. Am. Chem. Soc.*, **94**, 946 (1972); (d) J.A. Kemlo, T.M. Shepherd. *Chem. Phys. Lett.*, **47**, 158 (1977); (e) A. Harriman. *J. Chem. Soc., Faraday Trans.*, **2** (77), 1281 (1981); (f) H. Masuhara,

H. Shioyama, T. Saito, K. Hamada, S. Yasoshima, N. Mataga. *J. Phys. Chem.*, **88**, 5868 (1984); (g) S. Jayaramanu, A.S. Verkman. *Biophys. Chem*., **85**, 49 (2000).
[19] Rigaku Oxford Diffraction. *CrysAlisPro Software System, Version 1.171.40.23a*, Rigaku Corporation, Oxford, UK (2018).
[20] Bruker. *SAINT+*, Bruker AXS Inc., Madison, WI (2007).
[21] G.M. Sheldrick. *SHELXL-97, Program for X-ray Crystal Structure Refinement*, University of Göttingen, Germany (1997).
[22] Bruker. *APEX II*, Bruker AXS Inc., Madison, WI (2013).
[23] G.M. Sheldrick. *Acta Crystallogr, Sect. A: Found. Crystallogr.*, **64**, 112 (2008).
[24] L.J. Farrugia. *J. Appl. Crystallogr.*, **45**, 849 (2012).
[25] G.M. Sheldrick. *Acta Crystallogr., Sect. C: Struct. Chem.*, **71**, 3 (2015).
[26] C.F. Macrae, P.R. Edgington, P. McCabe, E. Pidcock, G.P. Shields, R. Taylor, M. Towler, J. van de Streek. *J. Appl. Crystallogr.*, **39**, 453 (2006).
[27] A.L. Spek. *Acta Crystallogr, Sect. D: Biol. Crystallogr*, **65**, 148 (2009).
[28] V. Vreshch. *J. Appl. Crystallogr.*, **44**, 219 (2011).
[29] (a) C.M. Reddy, K.A. Padmanabhan, G.R. Desiraju. *Cryst. Growth Des*., **6** (12), 2720 (2006); (b) C.M. Reddy, R.C. Gundakaram, S. Basavoju, M.T. Kirchner, K.A. Padmanabhan, G.R. Desiraju. *Chem. Commun*., **31**, 3945 (2005).
[30] R. Irshad, S. Asim, A. Mansha, Y. Arooj. *J. Fluoresc*., **33**, 1273 (2023).
[31] (a) Z. Hua, S. Gong, Y. Tian, H. Fu. *Chem. Commun*., **60**, 7246 (2024);(b) L. Yang, Y. Yu, J. Feng, J. Wu, L. Jiang, Y. Dan, Y. Qiu. *J. Photochem. Photobiol. A: Chem*., **350**, 103 (2018); (c) T.S. Sreena, A.K.V. Raj, P.P. Rao. Solid State Sci., **123**, 106783 (2022).
[32] K. Rurack. *Spectrochim. Acta, Part A*, **57**, 2161 (2001).
[33] (a) T. Chattopadhyay, A. Banerjee, K.S. Banu, E. Suresh, M. Netahji, G. Birarda, E. Zangrando, D. Das. *Polyhedron*, **27**, 2452 (2008);(b) C.D. Geddes. *Meas. Si. Technol.*, **12**, R53 (2001).
[34] M. Formica, V. Fusi, L. Florgi, M. Micheloni. *Coord. Chem. Rev.*, **256**, 170 (2012).
[35] J.K. Nath, A. Mondal, A.K. Powell, J.B. Baruah. *Cryst. Growth Des.*, **14**, 4735 (2014).
[36] Y. Guo, F. Cao, P. Qiu, Z. Wang. *J. Lumin*, **34**, 450 (2019).
[37] (a) F. Yang, Y. Ren, D. Li, F. Fu, G. Qi, Y. Wang. *J. Mol. Struct*., **892** (1–3), 283 (2008);(b) H. Song, S. Rajendiran, E. Koo, B.K. Min, S.K. Jeong, T.D. Thangadurai, S. Yoon. *J. Lumin*., **132** (11), 3089 (2012); (c) H. Zhao, D. Jia, J. Li, G.J. Moxey, C. Zhang. *Inorg. Chim. Acta*, **432**, 1 (2015); (d) W.M. Liao, C.J. Li, X.W. Wu, J.H. Zhang, Z. Wang, H.P. Wang, Y.N. Fan, M. Pan, C.Y. Su. *J. Mater. Chem. C.*, **6**, 3254 (2018).
[38] S. Pal, N. Chatterjee, P.K. Bharadwaj. *RSC Adv*., **4**, 26585 (2014).
[39] J.C. Deemsa, J.H. Reibenspiesb, H.-S. Leea, R.D. Hancocka. *Inorg. Chim. Acta*, **499**, 119181 (2020).
[40] N. Pandey, S. Pant, M.S. Mehata. *J. Lumin*, **38**, 1192 (2022).
[41] A. Gusev, E. Braga, Y. Baluda, M. Kiskin, M. Kryukova, N. Karaush-Karmazin, G. Baryshnikov, A. Kuklin, B. Minaev, H. Ågren, W. Linert. *Polyhedron*, **191**, 114768 (2020).